Soft Matter

# Diffusiophoresis in ionic surfactants: effect of micelle formation



| | |
|---|---|
| Journal: | *Soft Matter* |
| Manuscript ID | SM-ART-07-2018-001472.R1 |
| Article Type: | Paper |
| Date Submitted by the Author: | 30-Oct-2018 |
| Complete List of Authors: | Warren, Patrick; Port Sunlight Laboratory, Unilever Research<br>Shin, Sangwoo; University of Hawai'i at Manoa, Department of Mechanical Engineering<br>Stone, Howard; Princeton, Mechanical and Aerospace Engineering |
| | |

Journal Name

ARTICLE TYPE

Cite this: DOI: 10.1039/xxxxxxxxxx

# Diffusiophoresis in ionic surfactants: effect of micelle formation

Patrick B Warren,[a] Sangwoo Shin,[b] and Howard A Stone[c]

Received Date
Accepted Date

DOI: 10.1039/xxxxxxxxxx

www.rsc.org/journalname

We explore the consequences of micelle formation for diffusiophoresis of charged colloidal particles in ionic surfactant concentration gradients, using a quasi-chemical association model for surfactant self assembly. The electrophoretic contribution to diffusiophoresis is determined by re-arranging the Nernst-Planck equations, and the chemiphoretic contribution is estimated by making plausible approximations for the density profiles in the electrical double layer surrounding the particle. For sub-micellar solutions we find that a particle will typically be propelled down the concentration gradient, although electrophoresis and chemiphoresis are finely balanced and the effect is sensitive to the detailed parameter choices and simplifying assumptions in the model. Above the critical micelle concentration (CMC), diffusiophoresis becomes much weaker and may even reverse sign, due to the fact that added surfactant goes into building micelles and not augmenting the monomer or counterion concentrations. We present detailed calculations for sodium dodecyl sulfate (SDS), finding that the typical drift speed for a colloidal particle in a $\sim 100\,\mu\mathrm{m}$ length scale SDS gradient is $\sim 1\,\mu\mathrm{m\,s^{-1}}$ below the CMC, falling to $\lesssim 0.2\,\mu\mathrm{m\,s^{-1}}$ above the CMC. These predictions are broadly in agreement with recent experimental work.

The recent surge of interest in colloidal diffusiophoresis has been driven by the realisation that it is potentially a very common and widespread non-equilibrium colloidal transport mechanism, relevant for many physical phenomena and across many scientific fields.[1] The phenomenon was originally identified in the 1940s by Derjaguin and coworkers,[2] and revisited in the 1980s by Anderson, Prieve and others.[3–9] Much of the current focus has been directed towards diffusiophoresis in electrolyte gradients where significant effects additionally arise from the electric fields associated with diffuse liquid junction potentials (LJPs).[10–27] More recently, diffusiophoresis in polymer solutions,[28] and surfactant solutions,[18,29,30] has also been examined.

For ionic surfactants the problem combines elements of both electro-diffusiophoresis, and surfactant self-assembly. In a recent study it was noted that whilst diffusiophoresis approximately follows the normal rules in sub-micellar solutions, it is practically 'switched off' above the critical micelle concentration (CMC).[29] In our own work we confirmed that diffusiophoresis in sub-micellar surfactant solutions operates as a significant transport mechanism, relevant for example to pore-scale particulate soil removal in laundry detergency.[30] However we left open the question of what happens above the CMC.

Here we extend the standard theory of diffusiophoresis in electrolyte solutions to take account of micelle formation, basing our approach on earlier quasi-chemical association models that were successfully developed for surfactant diffusion.[31–33] Whilst not exactly 'switched off', we find that diffusiophoresis is significantly diminished or even reversed above the CMC, because added surfactant goes into building micelles and does not augment the monomer or counterion concentrations. We also note that for anionic surfactants there is a fine balance between electrophoresis in the LJP, and chemiphoresis due to osmotic pressure gradients in the electrical double layer (EDL) adjacent to the particle surface. This makes the results exquisitely sensitive to detailed parameter choices, and susceptible to errors arising from the simplifying assumptions in the models. Therefore we do not expect the present study will be the final word on this problem, and indeed at present experiment seems destined to be the ultimate arbiter in this complex situation.

Below, after introducing the problem and our notation, we shall set up the quasi-chemical association model for surfactant micelle formation, then compute the consequences for both electrophoresis in the LJP, and for chemiphoresis using plausible approximations for the ion density profiles in the EDL. For quantitative results we shall largely focus on sodium dodecyl sulfate (SDS), which is a well-characterised, prototypical, anionic surfactant for

[a] Unilever R&D Port Sunlight, Quarry Road East, Bebington, Wirral, CH63 3JW, UK; E-mail: patrick.warren@unilever.com
[b] Department of Mechanical Engineering, University of Hawaii at Manoa, Honolulu, Hawaii 96822, USA.
[c] Department of Mechanical and Aerospace Engineering, Princeton University, Princeton, New Jersey 08544, USA.

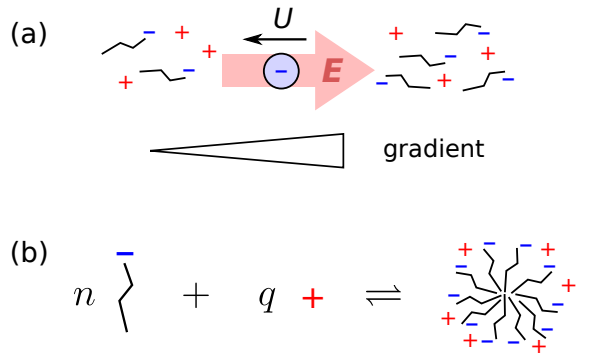


**Fig. 1** (a) Electrophoresis of a negatively-charged particle in an anionic surfactant concentration gradient: the counterions are more mobile and become slightly more spread out leading to a liquid junction potential and an accompanying electric field; this effect drives particle motion down the concentration gradient. (b) Schematic quasi-chemical association model for surfactant self assembly: $n$ monomers and $q$ counterions combine to make one micelle, of net charge $z = n - q$.

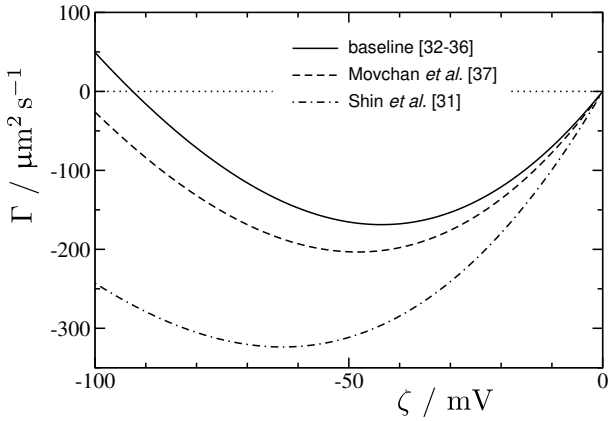


**Fig. 2** Sub-micellar diffusiophoretic drift coefficient for a negatively charged particle in SDS, from Eqs. (2)–(4). See Table 1 for the relevant diffusion coefficients.

which there is abundant physico-chemical data. In particular, for SDS the underpinning quasi-chemical association model is well tested, and the requisite parameters are readily available.

Importantly, we shall tune our approximations to the case where the charge on the particle (quantified by the $\zeta$-potential) has the *same sign* as the charge on the surfactant (*e. g.* negatively charged particles in anionic surfactants). This seems to be the practically relevant situation,[29] and corresponds to an underpinning assumption that the surfactant *ipso facto* is likely to be strongly adsorped onto the particle surface thereby overriding the bare charge. We shall further assume this adsorped surfactant has the sole effect of regulating the $\zeta$-potential and makes no direct contribution to phoretic transport.

Finally we shall assume the EDL is thin compared to the colloidal particle size. With this approximation, the diffusiophoretic drift velocity is independent of particle size and shape.[8] Since we are interested in surfactant concentrations around the CMC (typically a few mM) where the Debye length $\kappa^{-1} \lesssim 3\,\mathrm{nm}$, this restricts us to particle diameters $2a \gtrsim 500\,\mathrm{nm}$, *i. e.* $\kappa a \gtrsim 100$,[20,34] although we expect the trends to be preserved for smaller particles.

## 1 Sub-micellar diffusiophoresis

For electrolytes, there are two effects that combine to cause diffusiophoretic drift. The first as already mentioned arises from electrophoresis in the LJP. The sign of the LJP depends on the relative mobilities of the ions and the corresponding electric field can be in either direction. For example, in common rock salt (NaCl) the anion is more mobile than the cation and consequently electrophoresis of a negatively charged particle is up the salinity gradient (towards higher salt concentrations); in KCl the ion mobilities are almost equal and the LJP is very small; while in ionic surfactants the bulkier surfactant has a smaller mobility than the counterion so that electrophoresis of a like-charged particle is almost certainly down the concentration gradient (Fig. 1a).

The second contribution to diffusiophoresis arises from osmotic gradients within the EDL. Typically this effect drives motion up gradients since this reduces the interfacial free energy in the EDL. The chemiphoretic contribution can be viewed as a kind of wall-bounded Marangoni effect.[3]

Let us set up the notation in the context of the basic phenomenology. We define a diffusiophoretic drift coefficient $\Gamma$ which gives the velocity of a suspended colloidal particle in terms of the gradient of the logarithm of the electrolyte concentration,

$$\mathbf{U} = \Gamma \nabla \ln c\,. \tag{1}$$

With the above considerations this drift coefficient then naturally decomposes into electrophoretic and chemiphoretic contributions, as

$$\Gamma = \Gamma_e + \Gamma_c\,. \tag{2}$$

For simple electrolytes the standard theory gives[5,8]

$$\Gamma_e = \frac{\varepsilon_r \varepsilon_0}{\eta}\left(\frac{k_\mathrm{B}T}{e}\right)^2 \times \frac{e\zeta}{k_\mathrm{B}T}\,\beta\,, \tag{3a}$$

$$\Gamma_c = \frac{\varepsilon_r \varepsilon_0}{\eta}\left(\frac{k_\mathrm{B}T}{e}\right)^2 \times 4\ln\cosh\left(\frac{e\zeta}{4k_\mathrm{B}T}\right). \tag{3b}$$

In these, $\varepsilon_r$ and $\varepsilon_0$ are dielectric permittivities of the medium and vacuum, $\eta$ is the viscosity, $k_\mathrm{B}T$ is the thermal energy, $e$ is the basic unit of charge, $\zeta$ is the surface potential, and

$$\beta = \frac{D_2 - D_1}{D_1 + D_2} \tag{4}$$

is the diffusivity contrast in which $D_1$ and $D_2$ are the diffusion coefficients of the anion and cation respectively (see Table 1).

For water at room temperature (25°C), $k_\mathrm{B}T/e \approx 25\,\mathrm{mV}$, $\varepsilon_r\varepsilon_0/\eta \approx 0.8\,\mu\mathrm{m^2\,s^{-1}\,mV^{-2}}$, and the prefactor in the above $(\varepsilon_r\varepsilon_0/\eta)(k_\mathrm{B}T/e)^2 \approx 500\,\mu\mathrm{m^2\,s^{-1}}$. This sets the overall scale for the phenomenon; for example a salt gradient on a length scale $L \sim 100\,\mu\mathrm{m}$ gives rise to a diffusiophoretic drift velocity $\Gamma/L \sim 1$–$10\,\mu\mathrm{m\,s^{-1}}$; thus the time for a μm-sized colloidal particle to be propelled over this distance is of the order 10–100 s. This can be contrasted with the diffusion time $L^2/D_p \sim 10^4\,\mathrm{s}$ where $D_p \sim 1\,\mu\mathrm{m^2\,s^{-1}}$ is a typical diffusion coefficient for a μm-sized colloid.

**Table 1** Diffusion coefficients ($10^{-9}\,m^2\,s^{-1}$) for SDS monomers ($D_1$), counterions ($D_2$), and micelles ($D_m$). The baseline represents the consensus from the older literature whereas Movchan *et al.* and Shin *et al.* are representative of more recent experimental measurements. The $\beta$-parameter is from Eq. (4).

| | $D_1$ | $D_2$ | $D_m$ | $\beta$ |
|---|---|---|---|---|
| baseline, refs. 31– 35 * | 0.57 | 1.33 | 0.11 | 0.40 |
| Movchan *et al.*, ref. 36 | 0.52 | 1.33 | 0.10 | 0.44 |
| Shin *et al.*, ref. 30 | 0.39 | 1.33 | 0.10 | 0.55 |

*See also Table S1 in ref. 30

The marked difference signals that diffusiophoresis is potentially vastly more effective than diffusion in moving colloidal material. It is this feature that makes diffusiophoresis such an important non-equilibrium transport mechanism.

Below the CMC, we shall suppose (as others do) that the surfactant in solution exists as dissociated monomers and counterions and the above theory can be applied without further refinement.[29,30] One interesting and important consequence already mentioned for ionic surfactants is that chemiphoretic drift is almost surely in the opposite direction to electrophoresis in the LJP. Therefore the magnitude, and even direction, of the net drift is a sensitive function of the material properties. Additionally, the magnitude is considerably reduced from the above ball-park estimate, perhaps even by as much as a factor of ten, as provided in Fig. 2, which shows values based on measurements reported by different groups (Table 1). Nevertheless, diffusiophoresis still remains a potent transport process since the logarithmic dependence on the salt concentration in Eq. (3) leads to persistent effects well beyond what one would estimate from the bare diffusion time, such as salt trapping,[12] and long-lasting pore-scale particle removal.[30]

A related observation is that the dependence on the $\zeta$-potential is non-monotonic. This is demonstrated for SDS in Fig. 2 (see also Fig. 10). For example, for sub-micellar SDS solutions with baseline diffusion coefficients as in Table 1, the largest effect is at $\zeta \approx -45\,mV$ where $\Gamma \approx -170\,\mu m^2\,s^{-1}$; and $\Gamma$ becomes positive for $\zeta \lesssim -90\,mV$. We shall focus our calculations on $\zeta \approx -80\,mV$ since this is a typical value.[30] For this case, the baseline sub-micellar $\Gamma \approx -70\,\mu m^2\,s^{-1}$. To put this in perspective, an SDS gradient over a length scale $L \sim 100\,\mu m$ gives rise to a diffusiophoretic drift velocity $\Gamma/L \sim 1\,\mu m\,s^{-1}$.

## 2 Supra-micellar diffusiophoresis

As stated our main purpose is to generalise Eqs. (3)–(4) to include the effects of micelle formation for ionic surfactants. We note that Eqs. (3) predict that $\Gamma$ should be *independent* of concentration below the CMC; this is no longer to be expected to be the case in the presence of micelles, and indeed this is an outcome of the theory developed below.

Above the CMC, the system contains monomers, micelles and counterions, and should be treated as a ternary system albeit one which in which monomeric and micellar surfactant can equilibrate. This leads to a rich though manageable problem. In the following, the micelle kinetics shall be assumed fast (relaxation times typically $\lesssim 0.1\,s$) so that local equilibrium can be assumed.[32,37] Following much earlier work on the problem of surfactant diffusion,[31–33] the analysis will be done in the context of a simple quasi-chemical association model (see Fig. 1b). An important point to note is that to make sense of the physico-chemical observations it has long been established that in such a model one has to assume some fraction of counterions are 'bound' to the micelle. This is explicitly incorporated into the model.

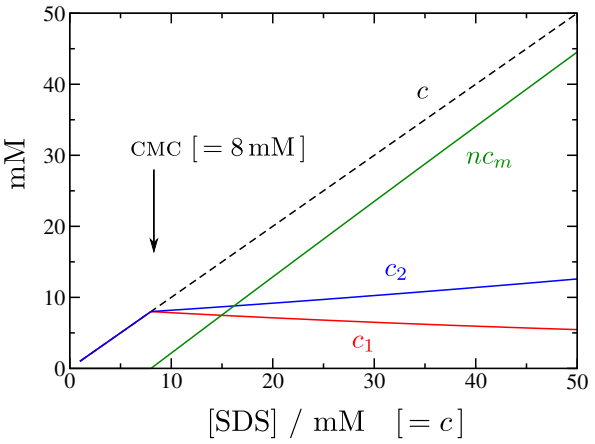


**Fig. 3** Monomer ($c_1$), counterion ($c_2$), and micellar surfactant ($nc_m$) concentrations for SDS, from the quasi-chemical association model with $n = 60$ and $q/n = 0.84$ (see Appendix A).

### 2.1 Quasi-chemical association model

Following Leaist,[33] let $c_1$ be the monomer surfactant concentration (number density), $c_2$ the free counterion concentration, and $c_m$ the micelle number density. Let the total surfactant concentration be $c$; this is also the total counterion concentration, assuming univalent surfactant ions and counterions. We suppose that $n$ surfactant monomers and $q$ counterions combine to form one micelle (Fig. 1b), so that a micelle has a net charge of magnitude $z = n - q$. For example, for SDS the consensus is $n \approx 60$ and $q/n \approx 0.84$.[31]

We have the following mass balances, and law of mass action,

$$c = c_1 + nc_m\,, \quad c = c_2 + qc_m\,, \quad c_m = Kc_1^n c_2^q\,. \tag{5}$$

In the last of these, $K$ is an equilibrium constant related to the CMC (see Appendix A). Since $c_1$, $c_2$ and $c_m$ are all supposed small (mM), we neglect corrections for non-ideality (activity coefficients) both here and in the Nernst-Planck equations below. Eqs. (5) are sufficient to determine $c_1$, $c_2$ and $c_m$ in terms of $c$, which we shall take to be the independent concentration variable. More details of the solution method and the relationship between $K$ and the CMC are given in Appendix A. For SDS the behaviour is shown in Fig. 3.

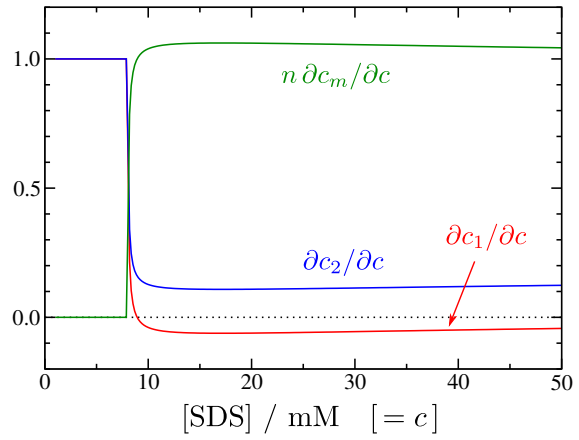


**Fig. 4** Gradient terms from Eqs. (6) corresponding to Fig. 3.

Eqs. (5) can be differentiated to find

$$\frac{\partial c_1}{\partial c} = \frac{c_1c_2 - zqc_1c_m}{c_1c_2 + q^2c_1c_m + n^2c_2c_m}\,, \tag{6a}$$

$$\frac{\partial c_2}{\partial c} = \frac{c_1c_2 + znc_2c_m}{c_1c_2 + q^2c_1c_m + n^2c_2c_m}\,, \tag{6b}$$

$$\frac{\partial c_m}{\partial c} = \frac{qc_1c_m + nqc_2c_m}{c_1c_2 + q^2c_1c_m + n^2c_2c_m}\,. \tag{6c}$$

These equations will be critical in the sequel. In the sub-micellar limit ($c_m \to 0$, $c_i \to c$ for $i = 1,2$), one has $\partial c_m/\partial c \to 0$ and $\partial c_i/\partial c \to 1$. Results for SDS are shown in Fig. 4.

### 2.2 Electrophoresis and the Nernst-Planck equations

Liquid junction potentials (LJPs) in electrolyte solutions arise because of a mismatch in ionic mobilities: in a concentration gradient the faster ions try to spread out more rapidly than the slower ions leading to a charge imbalance, which gives rise to a compensating electric field. The actual charge imbalance is miniscule, and to a very good approximation the LJP can be calculated assuming local charge neutrality.[38–42] In the present case this implies that the charge current vanishes.[43]

Leaist splits the problem into thermodynamic and mobility calculations (see Appendix B), but the end result can be reached perhaps more transparently and succinctly simply by rearranging the Nernst-Planck equations for the fluxes $\mathbf{J}_1$, $\mathbf{J}_2$ and $\mathbf{J}_m$, which correspond to the three solution species. This also gives direct access to the electric field (LJP). For this problem, the Nernst-Planck equations for the monomeric surfactant molecules (charge $-1$), counterions (charge $+1$), and micelles (charge $-z$) are respectively

$$\mathbf{J}_1 = -D_1(\nabla c_1 - c_1\nabla\psi)\,, \tag{7a}$$

$$\mathbf{J}_2 = -D_2(\nabla c_2 + c_2\nabla\psi)\,, \tag{7b}$$

$$\mathbf{J}_m = -D_m(\nabla c_m - zc_m\nabla\psi)\,. \tag{7c}$$

In these, $D_1$, $D_2$ and $D_m$ are diffusion coefficients, and $\psi = e\phi/k_BT$ is the dimensionless electrostatic potential. As mentioned, the charge current vanishes,[43]

$$\mathbf{I} = \mathbf{J}_2 - \mathbf{J}_1 - z\mathbf{J}_m = 0\,. \tag{8}$$

This constraint can be used to solve for $\nabla\psi$ in terms of the concentration gradients. It is convenient to write this as $\nabla\psi = (\partial\psi/\partial c)\nabla c$ where

$$\frac{\partial\psi}{\partial c} = \frac{D_1\frac{\partial c_1}{\partial c} - D_2\frac{\partial c_2}{\partial c} + zD_m\frac{\partial c_m}{\partial c}}{c_2D_1 + c_2D_2 + z^2c_mD_m}\,. \tag{9}$$

This can now be used to eliminate the $\nabla\psi$ terms from the Nernst-Planck equations, and in combination with Eqs. (6) to obtain $\mathbf{J}_1$, $\mathbf{J}_2$, $\mathbf{J}_m$ and $\nabla\psi$, as a function of the overall concentration gradient $\nabla c$ (or $\nabla\ln c$).

The conservation law for the total surfactant concentration is $\partial c/\partial t + \nabla\cdot\mathbf{J} = 0$ where $\mathbf{J} = \mathbf{J}_1 + n\mathbf{J}_m$. With the above results we find that $\mathbf{J} = -D_c(c)\nabla c$ where

$$D_c = D_1\frac{\partial c_1}{\partial c} + nD_m\frac{\partial c_m}{\partial c} - (c_1D_1 + nzc_mD_m)\frac{\partial\psi}{\partial c}\,. \tag{10}$$

The concentration-dependent collective diffusion coefficient that results from injecting Eqs. (6) into Eq. (10) is reported in Eq. (11a) below. Bearing in mind the redundancy $n = q + z$, it is the same as described previously.[32,33] One can readily check that in the sub-micellar limit it reduces to $D_c = 2D_1D_2/(D_1 + D_2)$, thus recovering the familiar ambipolar diffusion coefficient.

In the context of diffusiophoresis we are obviously interested in the electric field $\mathbf{E} = -(k_BT/e)\nabla\psi$. To quantify this, we generalise the $\beta$ factor that appears in Eqs. (3), defining it such that $e\mathbf{E}/k_BT = \beta(c)\nabla\ln c$, or $\beta = -c\,\partial\psi/\partial c$. Fully expanded, this concentration-dependent $\beta$-parameter is given in Eq. (11b) below. In the sub-micellar limit it reduces to $\beta = (D_2 - D_1)/(D_1 + D_2)$, thus is the correct generalisation of the familiar result.

Our results are summarised in the following expressions, although for practical calculations it is just as easy to work with Eqs. (6), (9), and (10):

$$D_c(c) = \frac{(c_1 + c_2 + z^2c_m)(c_1c_2D_1D_2 + q^2c_1c_mD_1D_m + n^2c_2c_mD_2D_m)}{(c_1c_2 + q^2c_1c_m + n^2c_2c_m)(c_1D_1 + c_2D_2 + z^2c_mD_m)}\,, \tag{11a}$$

$$\beta(c) = c\,\frac{c_1c_2(D_2 - D_1) + qzc_1c_m(D_1 - D_m) + nzc_2c_m(D_2 - D_m)}{(c_1c_2 + q^2c_1c_m + n^2c_2c_m)(c_1D_1 + c_2D_2 + z^2c_mD_m)}\,. \tag{11b}$$

Eq. (11b) is to be used with Eq. (3a) to obtain the electrophoretic contribution to the drift coefficient $\Gamma_e$. To recapitulate, subscript '1' refers to the monomeric surfactants, '2' to the counterions, and '$m$' to the micelles, in these expressions. Note that Eq. (11a) is identical to Eq. (25) in ref. 33.

### 2.3 Chemiphoresis and the Poisson-Boltzmann equation

To estimate the chemiphoretic contribution to the drift, we start with a general expression for the diffusio-osmotic wall slip veloc-

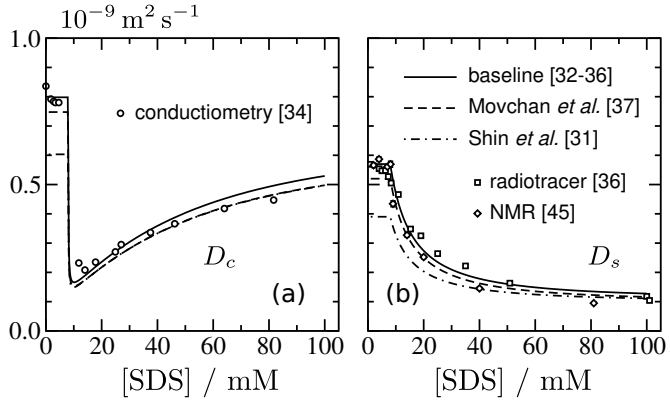


**Fig. 5** (a) Collective, and (b) self diffusion coefficients for SDS. Lines are from the quasi-chemical association model with diffusion coefficients from Table 1. Data points are from (a) conductiometry [ref. 33; circles], and (b) radiotracer [ref. 35; squares] and NMR [ref. 44; diamonds].

ity in the presense of multiple solute gradients,[3]

$$\mathbf{v}_s = -\frac{k_\mathrm{B}T}{\eta}\sum_i \Big\{\int_0^\infty y\,dy\,\Big(\frac{c_i(y)}{c_i(\infty)}-1\Big)\Big\}\nabla_s c_i\,. \tag{12}$$

In this equation, $y$ is the direction normal to the wall and $\nabla_s$ is the projection of the gradient operator parallel to the wall.[8] In our problem there are three components, and we assume that the concentration profiles in the EDL are governed by a common dimensionless electrostatic potential $\psi(y)$ normal to the wall. Under the thin EDL approximation we can transpose this into a colloidal drift velocity,[5,8]

$$\mathbf{U} = \frac{k_\mathrm{B}T}{\eta}\Big[\Big\{\int_0^\infty y\,dy\,(e^{\psi}-1)\Big\}\nabla_s c_1 + \Big\{\int_0^\infty y\,dy\,(e^{-\psi}-1)\Big\}\nabla_s c_2 + \Big\{\int_0^\infty y\,dy\,(e^{z\psi}-1)\Big\}\nabla_s c_m\Big]\,. \tag{13}$$

We now further assume that the surface is negatively charged (as appropriate for an anionic surfactant) and that $\psi$ can be taken from the solution to the Poisson-Boltzmann equation (PBE) for the small ions only,

$$\psi = 2\ln\Big(\frac{1+Ce^{-\kappa y}}{1-Ce^{-\kappa y}}\Big)\,, \tag{14}$$

where $C=\tanh(\frac{1}{4}\psi_0)$, $\psi_0 = e\zeta/k_\mathrm{B}T$ is the dimensionless $\zeta$-potential, and $\kappa$ is the inverse Debye length, which will be discussed further below.

The first two integrals in Eq. (13) can now be done analytically, and the last approximated by assuming that micelles are excluded from an inner region $0<y\lesssim H$ where $|z\psi|\gg 1$, and treating the outer region analytically where the far-field PBE solution can be used. More details are given in Appendix C. The final result is

$$\Gamma_c = \frac{ck_\mathrm{B}T}{\eta\kappa^2}\Big[4\ln\tfrac{1}{2}(1+e^{\psi_0/2})\frac{\partial c_1}{\partial c} + 4\ln\tfrac{1}{2}(1+e^{-\psi_0/2})\frac{\partial c_2}{\partial c} - (1+\kappa H+\tfrac{1}{2}\kappa^2H^2)\frac{\partial c_m}{\partial c}\Big]\,, \tag{15}$$

where $\kappa H = \ln(4\alpha z\tanh\frac{1}{4}|\psi_0|)$ and $\alpha\approx 0.713$ is fine-tuned to match with the numerical results (Fig. 14). Injecting the individual gradients from Eq. (6) into Eq. (15) yields a complete solution for $\Gamma_c$. In the sub-micellar limit Eq. (15) goes over to Eq. (3b) since one can show $\ln\frac{1}{2}(1+e^{\psi_0/2})+\ln\frac{1}{2}(1+e^{-\psi_0/2}) = 2\ln\cosh\frac{1}{4}\psi_0$.

Note that since $\psi_0<0$ the first and third terms in Eq. (15) are negative and the middle term is positive (see Fig. 13). This accords with the fact that the anionic surfactant monomers and micelles are expelled from the EDL, whereas the cationic counterions are attracted into it.

The inverse Debye screening length $\kappa$ that features in the PBE solution deserves further discussion. Formally, this is the screening length in a salt reservoir containing only the small ions, in a Donnan equilibrium with the bulk.[45,46] Supposing the Donnan potential is $\psi_D$, then $c_1 = c_R\exp(\psi_D)$ and $c_2 = c_R\exp(-\psi_D)$ where $c_R$ is the ion concentration in the reservoir. From these, $c_R=\sqrt{c_1c_2}$, $\psi_D=\frac{1}{2}\ln(c_1/c_2)$, and formally $\kappa_R^2 = 2e^2c_R/(\varepsilon_r\varepsilon_0k_\mathrm{B}T)$. In the PBE the zero-point of the potential is defined to be in this same salt reservoir so that one should have $\psi\to\psi_D$ in the bulk. Whilst this is not exactly satisfied (as will be discussed in the next paragraph), linearising the PBE about this bulk value yields an effective screening length $\kappa^2=\kappa_R^2\cosh\psi_D$.[45] This amounts to setting $\kappa^2 = e^2(c_1+c_2)/(\varepsilon_r\varepsilon_0k_\mathrm{B}T)$. Taking this into consideration the prefactor in Eq. (15) is

$$\frac{ck_\mathrm{B}T}{\eta\kappa^2} = \frac{\varepsilon_r\varepsilon_0}{\eta}\Big(\frac{k_\mathrm{B}T}{e}\Big)^2\times\frac{c}{c_1+c_2}\,. \tag{16}$$

In the sub-micellar limit the last factor is $1/2$.

As remarked, the PBE solution in Eq. (14) does not actually satisfy $\psi\to\psi_D$ in the bulk (in fact it satisfies $\psi\to 0$), and thus does not strictly qualify according to the rules discussed in the preceding paragraph. In fact, unless one incorporates the background charge density of the micelles into the PBE,[46] a non-vanishing Donnan potential is incompatible with the requirement that the bulk electric field vanishes ($d\psi/dy\to 0$ as $y\to\infty$); essentially as a consequence of Gauss' law. One could resolve this at the expense of numerically integrating the PBE, but for present purposes we shall take Eq. (14) as a reasonable approximation as long as the Donnan potential is not too large. Calculations for SDS for instance indicate that $|\psi_D|\lesssim 10\,\mathrm{mV}$ for $c\lesssim 50\,\mathrm{mM}$ (note $\psi_D$ vanishes for sub-micellar solutions).

## 3 Results

Figures 5–10 show results for SDS, with a variety of assumptions for the underlying parameters. Let us first discuss the diffusion coefficients. Table 1 shows a selection of the underlying monomer ($D_1$), counterion ($D_2$), and micelle ($D_m$) diffusion coefficients that have been entertained in the literature. The first row summarises the older literature (see also Table S1 in ref.[30]), and is our baseline.[31–33,35,47] A reduced value of $D_1$ was recently proposed by Movchan *et al.* who note that $D_1$ declines by about 10% going from the infinite dilution limit to the CMC.[36] They attribute this to deviations from ideal solution behavior, and argue that the value at the CMC better captures the physical chemistry; this gives the second row in Table 1. Finally, the third row corresponds to

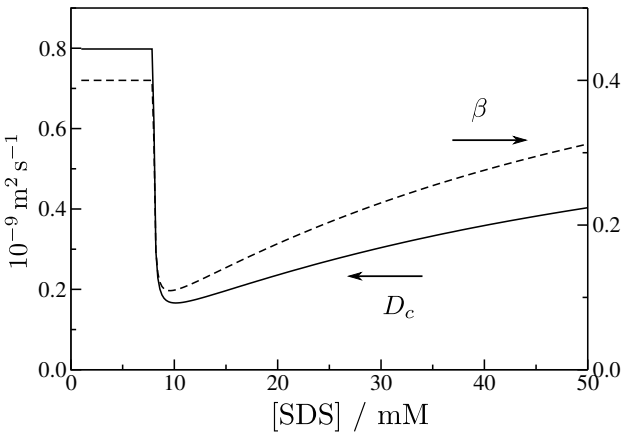


**Fig. 6** Collective diffusion coefficient $D_c$ (left axis), and $\beta$-parameter (right axis), using SDS baseline parameters from Table 1.

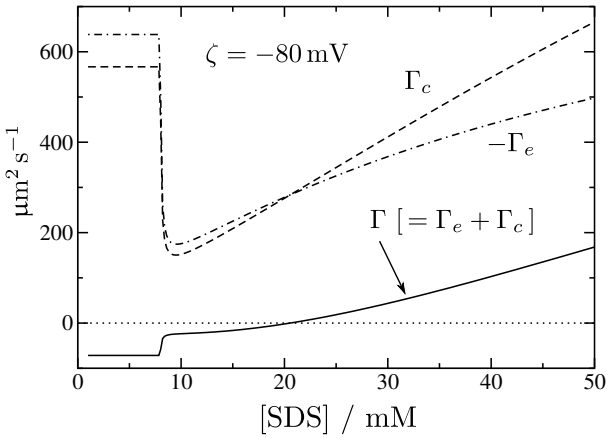


**Fig. 7** Diffusiophoretic drift coefficient in SDS broken down into electrophoretic and chemiphoretic contributions, for $\zeta = -80\,\mathrm{mV}$.

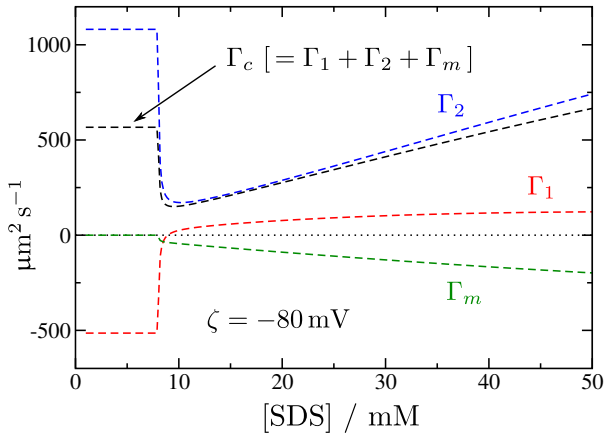


**Fig. 8** Chemiphoretic drift coefficient in SDS further broken down into contributions from individual solution species, for $\zeta = -80\,\mathrm{mV}$.

values which best fit our recent experiments on colloidal diffusiophoresis in SDS solutions.[30]

Collective ($D_c$) and self ($D_s$) (or tracer) diffusion coefficients calculated from the model are shown in Fig. 5, compared to some of the available experimental data.[33,35,44] The most noticeable phenomenon is the precipitous drop in $D_c$ at the CMC. The reason for this (Fig. 11) is that the chemical potential gradient flattens almost to zero above the CMC.[33] Less prominent, but puzzling to the early investigators, is the steady increase in $D_c$ with overall surfactant concentration above the CMC. As was realised at the time,[31–33] the explanation lies in the electrostatic coupling contained in the Nernst-Planck equations, combined with the evolving solution composition above the CMC that is captured by the quasi-chemical association model (Fig. 12). We see that the model captures this behavior very effectively. The effect of changing $D_1$ is fairly small and all results remain consistent with the experimental data (Fig. 5a).

In the quasi-chemical association model, the self diffusion coefficient is given as a weighted average $D_s = (1-\alpha)D_1 + \alpha D_m$ where $\alpha$ is the mole fraction of micellar surfactant (see Appendix A). Fig. 5b compares this to radiotracer[35] and NMR[44] experiments. Again, the agreement is rather good, though the dependence on $D_1$ becomes more pronounced and arguably the final row in Table 1 that derives from our own diffusiophoresis experiments is at odds with the self diffusion data. This will be touched on later.

The concentration-dependent $\beta(c)$, shown in Fig. 6, displays similar behavior to $D_c$, essentially for the same reasons but this time more deeply intertwined by Eq. (9) with the behavior of the individual gradients in Eqs. (6). The $\beta$-parameter governs the magnitude and direction of the electric field associated with the diffuse LJP, and is a solution property independent of the presence of tracer colloidal particles. The theory thus indicates that the LJP is significantly diminished above the CMC (for a given concentration gradient) and the electrophoretic drift coefficient $\Gamma_e$ is likewise diminished. This is shown in Fig. 7. Note that altering the diffusion coefficients does not affect the micellar equilibrium, and therefore does not affect the chemical potential or the gradient terms, but it *does* affect the LJP. Thus the electrophoretic component of diffusiophoresis is not solely governed by the surfactant chemical potential gradient.

Figure 7 also shows the chemiphoretic drift coefficient $\Gamma_c$ computed from Eqs. (15) and (16), and the net drift coefficient $\Gamma$. We see that the behavior of $\Gamma_c$ essentially mirrors that of $\Gamma_e$, but is of the opposite sign. The effect is again traceable to the behavior of the underpinning gradient terms. The chemiphoretic drift can be broken down into individual contributions from the different solution species, shown in Fig. 8. Inspecting these curves we see that even within the chemiphoretic drift calculation there is some partial cancellation of the individual contributions.

The net overall drift coefficient $\Gamma$ shown in Fig. 7 is considerably smaller than the individual contributions, which almost cancel each other. Compared to the behavior in sub-micellar solutions, the prediction is that diffusiophoresis declines significantly (by a factor 3–5) at the CMC, and then exhibits a slow variation with surfactant concentration above the CMC. At higher concentrations, $\Gamma$ may change sign and grow in magnitude again. This happens with the baseline parameter set for $c \gtrsim 20\,\mathrm{mM}$.

The remaining plots demonstrate these overall conclusions are robust against parameter variations, whilst providing further insight into the delicate balance of contributions. Fig. 9 shows the

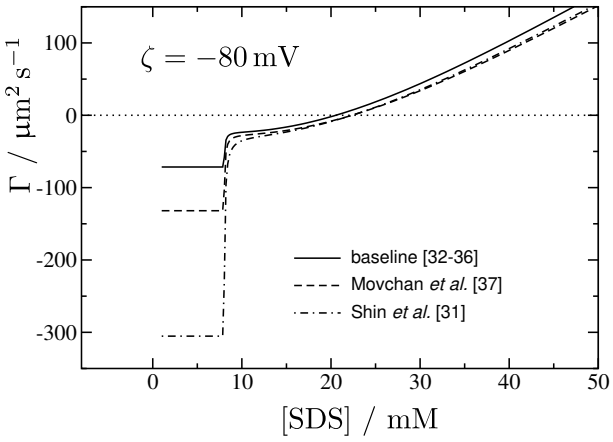


**Fig. 9** Effect on $\Gamma$ of varying diffusion coefficients (see Table 1).

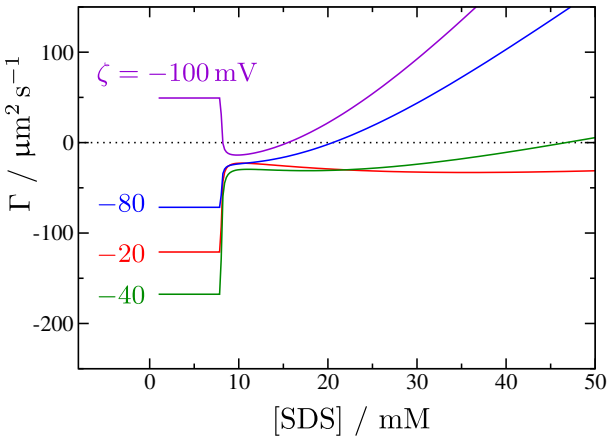


**Fig. 10** Effect on $\Gamma$ of varying the $\zeta$-potential. Note the striking non-monotonic trends.

effect of changing the diffusion coefficients from the baseline, keeping $\zeta = -80\,\mathrm{mV}$. Fig. 10 shows the effect of changing the $\zeta$-potential, for the baseline diffusion model. In all cases the overall magnitude of the drift coefficient falls abruptly at the CMC, then changes more slowly above the CMC and in some cases changes sign at concentrations typically several times the CMC. Just as for the collective diffusion coefficient, these trends reflect the behaviour of the underlying individual species gradients (Fig. 4).

## 4 Discussion

Overall, our calculations are in broad agreement with the existing experimental evidence for diffusiophoresis in surfactant solutions.[29,30] In particular for sub-micellar solutions we find that a colloidal particle will typically be propelled *down* a surfactant concentration gradient, assuming the surfactant also controls the surface charge of the particle. The basic mechanism is electrophoresis in the electric field associated with the liquid junction potential (Fig. 1a). This overcomes a slightly weaker opposing chemiphoretic drift arising from osmotic gradients in the EDL. As a result the net drift speed is considerably smaller than would be found for instance in an electrolyte gradient in which these contributions were not opposed. For example, in an SDS gradient over a length scale $\sim 100\,\mu\mathrm{m}$, the diffusiophoretic drift speed would be of the order $1\,\mu\mathrm{m\,s}^{-1}$ down the gradient, which can be compared to a speed of order $10\,\mu\mathrm{m\,s}^{-1}$ *up* a comparable NaCl gradient. In sub-micellar SDS concentration gradients, such drift speeds ($\sim 1\,\mu\mathrm{m\,s}^{-1}$) are in accord with recent measurements.[29,30]

At the critical micelle concentration, the prediction is that the diffusiophoretic drift coefficient abruptly drops, perhaps by a factor 3–5, and subsequently varies slowly with increasing concentration above this point. It may even vanish and change sign, before growing in magnitude again. Again, this response is roughly in accord with experimental observations of Nery-Azevedo *et al.*, although we predict a remnant drift coefficient whereas they find diffusiophoretic drift is practically absent. They also note a considerable discrepancy between the measured and calculated drift coefficient in sub-micellar solutions, where the theoretical situation should be relatively unambiguous. We now make some remarks on this aspect.

The obvious point is that the net drift coefficient is extraordinarily sensitive to some of the parameters in the problem, in particular the monomer diffusion coefficient $D_1$ and the surface $\zeta$-potential. This is shown in Fig. 2, and Figs. 9–10. For example a mere 5% decrease in $D_1$ increases the sub-micellar drift coefficient $\Gamma$ by $\approx 50\%$ (Fig. 2). Similarly increasing $|\zeta|$ by only 5 mV is enough to shrink $|\Gamma|$ by $\approx 35\%$. Thus, one could easily accommodate the deviations observed by Nery-Azevedo *et al.* with small changes to the model parameters. However this may be over-interpreting the theory as by the same consideration the results must also be sensitive to the underpinning approximations and assumptions in the model. We now list some of these.

First, the thin EDL approximation may be questioned since finite-size effects in diffusiophoresis may be unexpectedly significant even for micron-sized particles.[20,34] Also, Nery-Azevedo *et al.* mention polarization effects in the EDL although this seems to take the predictions in the wrong direction.[8,48] Another place where the theory may go wrong is in the detailed treatment of the EDL, for which Poisson-Boltzmann theory may be inadequate. Certainly, the assumption that the micelles are excluded from the relevant region in the EDL, and do not contribute to the screening, requires more careful examination in future work.

Another possible source of error lies in the assumption of ideal solution behavior. This is clearly an area for concern since surfactants are unlikely to be well-behaved in this respect, and indeeed the 10% decrease in $D_1$ at the CMC compared to the infinite dilution limit has been attributed to this effect.[36] As we have seen, a small correction affecting $D_1$ can have large consequences for diffusiophoresis. This may also be behind the discrepancy between the best-fit parameters for our diffusiophoresis experiments and the measured self diffusion coefficient.

These problems look formidable, but are hiding a potentially interesting opportunity. Note from Figs. 2 and 10 that the dependence on the $\zeta$-potential is quite significantly non-monotonic, and the theory predicts perhaps counterintuitively the *largest* effects may arise at *intermediate* surface charge. Since this also depends rather sensitively on surfactant adsorption, it offers a tantalising possibility to tune the surfactant and particle surface

chemistry to favour or disfavour diffusiophoresis under specific conditions. Obviously, given the parlous state of the theory, this would require detailed experimental validation, making inexpensive high-throughput methods to characterise phoretic transport rather desirable. We have already investigated this to some extent in the context of developing low-cost $\zeta$-potentiometry.[22]

Overall we can only claim to have taken the first steps towards building a theory of diffusiophoresis in surfactant solutions. Nevertheless we hope the present study will act as a spur to further investigations and experiments. One aspect that could rather easily be addressed though is the effect of the CMC on colloidal transport in dead-end capillaries. For this, the expression for the collective diffusion coefficient in Eq. (11a) can be used to obtain a time-dependent surfactant concentration profile, then the theory developed thus far can be used to predict colloidal trajectories as in our earlier work.[30] Whilst we must leave the detailed calculations for a future publication, we can anticipate that the precipitous drop in the surfactant diffusion coefficient above the CMC (Figs. 5a and 6) is likely to lead to a *shrinking core* of supramicellar surfactant in the case that one starts off with a high surfactant concentration inside a dead-end capillary. Then, colloidal particles will be expelled as they drift slowly into the sub-micellar region where diffusiophoresis is strongest. When finally the surfactant content falls everywhere below the CMC, the logarithmic dependence in Eq. (1) ensures continued persistent particle removal as established in our earlier work.[30] Thus we expect that even starting above the CMC, diffusiophoresis will remain a potent transport mechanism for particle removal from surfactant-laden dead-end capillaries.

## Conflicts of interest

PBW declares a substantive ($>$ \$10k) stock holding in Unilever PLC.

## Acknowledgements

HAS thanks the NSF for partial support via grant CBET-1702693.

## A Solution of association model

We summarise the solution of Eqs. (5) for $c_1$, $c_2$, and $c_m$, given the overall surfactant concentration $c$, in the limit of large aggregation number ($n \gg 1$). This is essentially the charged pseudophase model of Shinoda and later workers.[49–51] To proceed, write $nc_m = \alpha c$ so that $\alpha$ is the mole fraction of surfactant incorporated into micelles, and write $\theta = q/n$ for the fractional counterion binding. Then $c_1 = (1-\alpha)c$ and $c_2 = (1-\alpha\theta)c$, and the law of mass action becomes

$$(1-\alpha)(1-\alpha\theta)^\theta = k\alpha^\varepsilon c^{\varepsilon-1-\theta} \tag{17}$$

where $\varepsilon = 1/n$ is small, and $k$ is a constant related to $K$.

Note that $1-\alpha^\varepsilon = 1-e^{\varepsilon\ln\alpha} \approx -\varepsilon\ln\alpha \ll 1$ as long as $\alpha \gg O(e^{-n})$. This means that for $\varepsilon \to 0$ the behavior of Eq. (17) can be divided into two regimes, as

$$\begin{aligned} 1 &\approx k\alpha^\varepsilon c^{-1-\theta} && \alpha \lesssim O(e^{-n}), \\ (1-\alpha)(1-\alpha\theta)^\theta &\approx kc^{-1-\theta} && \alpha \gg O(e^{-n}). \end{aligned} \tag{18}$$

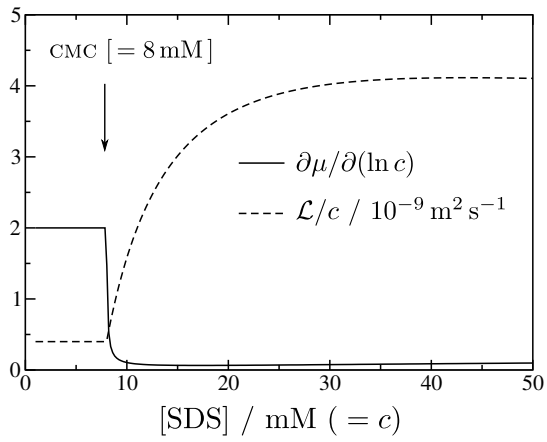


**Fig. 11** Dimensionless chemical potential gradient, and Onsager coefficient (generalised mobility), in Leaist's approach to calculating the collective diffusion coefficient for SDS.[33]

The two regimes are joined at $c = c_0$ where the right hand sides overlap, thus $1 = kc_0^{-1-\theta}$. This determines the CMC ($c_0$). In these terms one has

$$\begin{aligned} \alpha &\approx 0 && c < c_0, \\ (1-\alpha)(1-\alpha\theta)^\theta &\approx (c_0/c)^{1+\theta} && c > c_0. \end{aligned} \tag{19}$$

The mole fraction $\alpha(c)$ thus defined is continuous and piece-wise smooth, and in practical terms provides an excellent approximation for the exact solution of Eq. (17). Although the second of Eqs. (19) is implicit for $\alpha$, it is straightforward to solve numerically using a standard numerical root-finding toolbox (just about any initial guess $\alpha \in [0,1]$ should work). Once $\alpha(c)$ is determined, $(c_1, c_2, c_m)$ follow straightforwardly.

## B Leaist diffusion model

We make some comments on the approach adopted by Leaist in which first the chemical potential gradient $\nabla\mu$ is calculated, then related to the flux by $\mathbf{J} = -\mathscr{L}\nabla\mu$ where the Onsager coefficient $\mathscr{L}$ is a generalised mobility.[33] For notational simplicity in this Appendix we will work in units where $k_\mathrm{B}T = 1$. Note that it is impossible to extract $\nabla\psi$ in this approach, without injecting some additional information from the Nernst-Planck equations.

To get a handle on the thermodynamics it is convenient to start with the free energy of micellar association,

$$f = c_1(\ln c_1 - 1) + c_2(\ln c_2 - 1) + c_m(\ln c_m - 1) + gc_m. \tag{20}$$

The first three terms are ideal solution free energies, and the last is the free energy $g$ associated with assembling a micelle. This leads to the following chemical potentials,

$$\mu_1 = \ln c_1, \quad \mu_2 = \ln c_2, \quad \mu_m = \ln c_m + g. \tag{21}$$

The density variables $(c_1, c_2, c_m)$ are constrained by constancy of $c_1 + nc_m$ and $c_2 + qc_m$. Constrained minimisation of the free energy then reveals

$$\mu_m = n\mu_1 + q\mu_2. \tag{22}$$

This recovers the law of mass action as in the last of Eqs. (5), with

$K = e^{-g}$. Next,

$$\begin{aligned} df &= \mu_1\, dc_1 + \mu_2\, dc_2 + \mu_m\, dc_m \\ &= \mu_1\, dc_1 + \mu_2\, dc_2 + (n\mu_1 + q\mu_2)\, dc_m \\ &= \mu_1 (dc_1 + n\, dc_m) + \mu_2 (dc_2 + q\, dc_m) \\ &= \mu_1\, dc + \mu_2\, dc = (\mu_1 + \mu_2) dc\,, \end{aligned} \tag{23}$$

so that we identify

$$\mu \left( = \frac{\partial f}{\partial c} \right) = \mu_1 + \mu_2 = \ln(c_1 c_2)\,. \tag{24}$$

This same result can also be derived somewhat more laboriously by differentiating Eq. (20) and making use of Eq. (22) and Eqs. (6). The result for SDS is shown in Fig. 12. It is then easy to prove from Eqs. (6) that

$$\frac{\partial \mu}{\partial c} = \frac{c_1 + c_2 + z^2 c_m}{c_1 c_2 + q^2 c_1 c_m + n^2 c_2 c_m}\,. \tag{25}$$

This is the thermodynamic factor in Leaist's approach.

To get to the Onsager coefficient we rewrite the Nernst-Planck equations in terms of *electrochemical* potentials,

$$\begin{aligned} &\mathbf{J}_1 = -c_1 D_1 \nabla \tilde{\mu}_1\,, \quad \mathbf{J}_2 = -c_2 D_2 \nabla \tilde{\mu}_2\,, \\ &\mathbf{J}_m = -c_m D_m \nabla \tilde{\mu}_m\,, \end{aligned} \tag{26}$$

where

$$\tilde{\mu}_1 = \mu_1 - \psi\,, \quad \tilde{\mu}_2 = \mu_2 + \psi\,, \quad \tilde{\mu}_m = \mu_m - z\psi\,. \tag{27}$$

The two (charge neutral) relations in Eqs. (22) and (24) can also be written in these terms, as $\mu = \tilde{\mu}_1 + \tilde{\mu}_2$ and $\tilde{\mu}_m = n\tilde{\mu}_1 + q\tilde{\mu}_2$. Combining these with the zero current constraint $\mathbf{J}_1 + z\mathbf{J}_m = \mathbf{J}_2$ yields the fluxes in terms of $\nabla\mu$. Finally, defining $\mathbf{J} = \mathbf{J}_1 + n\mathbf{J}_m$ as before, one finds $\mathbf{J} = -\mathscr{L}\nabla\mu$ where

$$\mathscr{L} = \frac{c_1 c_2 D_1 D_2 + q^2 c_1 c_m D_1 D_m + n^2 c_2 c_m D_2 D_m}{c_1 D_1 + c_2 D_2 + z^2 c_m D_m}\,. \tag{28}$$

This is the Onsager coefficient. Since $\mathbf{J} = -\mathscr{L}\nabla\mu = -\mathscr{L}(\partial\mu/\partial c)\nabla c$, the overall diffusion coefficient is the product of the two factors in Eqs. (25) and (28). This recovers Eq. (11a) (equivalently Eq. (25) in ref. 33). Results for SDS (partly non-dimensionalised by factors of $c$) are shown in Fig. 11.

## C Chemiphoresis calculation

We present some more details of the Poisson-Boltzmann equation (PBE) and the integrals that appear in the chemiphoretic contribution. It will be convenient to work in terms of the reduced height $u = \kappa y$, and pull out a common factor $1/\kappa^2$ from the integrals in Eq. (13).

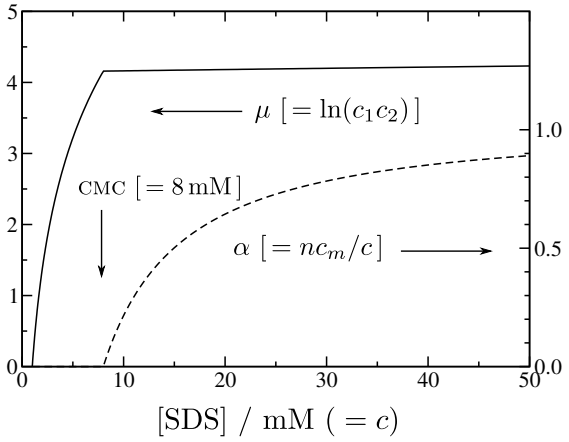


**Fig. 12** Chemical potential $\mu$ (in units of $k_B T$) and mole fraction $\alpha$ of micellar surfactant for SDS, corresponding to Figs. 3 and 4.

### C.1 Poisson-Boltzmann equation

We have to solve $d^2\psi/dy^2 - \kappa^2 \sinh\psi = 0$, or in terms of the reduced height

$$\frac{d^2\psi}{du^2} = \sinh\psi\,. \tag{29}$$

The boundary conditions are $\psi \to \psi_s$ at $u \to 0$ and $d\psi/du \to 0$ at $u \to \infty$. Whilst this is a textbook exercise,[52] the intermediate results facilitate the evaluation of the integrals in Eq. (13). As a first step multiply Eq. (29) through by $d\psi/du$ and integrate to find

$$\frac{1}{2}\left(\frac{d\psi}{du}\right)^2 = \cosh\psi - 1 = 2\sinh^2 \tfrac{1}{2}\psi\,. \tag{30}$$

The constant of integration has been chosen to correspond to $d\psi/du \to 0$ at $u \to \infty$. Next, it is the negative root of Eq. (30) that is required, thus

$$\frac{d\psi}{du} = -2\sinh \tfrac{1}{2}\psi\,. \tag{31}$$

Again, this integrates,

$$2\ln\tanh \tfrac{1}{4}\psi = -2u + \text{constant}\,, \tag{32}$$

or

$$\tanh \tfrac{1}{4}\psi = Ce^{-u} \tag{33}$$

where $C = \tanh \frac{1}{4}\psi_0$ as advertised. If we had made the wrong choice of sign in Eq. (31), this would have blown up as $e^u$ in the relevant half-space $u > 0$. Using the standard expression for the inverse hyperbolic tangent gives Eq. (14), in the main text.

### C.2 Concentration profile integrals

We use the above results to calculate the integrals in Eq. (13), which we write in dimensionless terms as

$$I_{1,2} = \int_0^\infty u\, du\, (e^{\pm\psi} - 1)\,, \quad I_m = \int_0^\infty u\, du\, (e^{z\psi} - 1)\,. \tag{34}$$

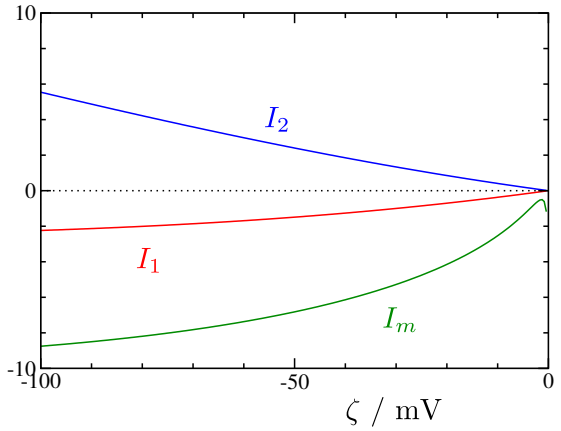


**Fig. 13** The individual integrals in Eqs. (34) as a function of the wall $\zeta$-potential, for SDS micelle charge $z = 9.6$. The downturn in $I_m$ just visible as $\zeta \to 0$ is an artefact (see text).

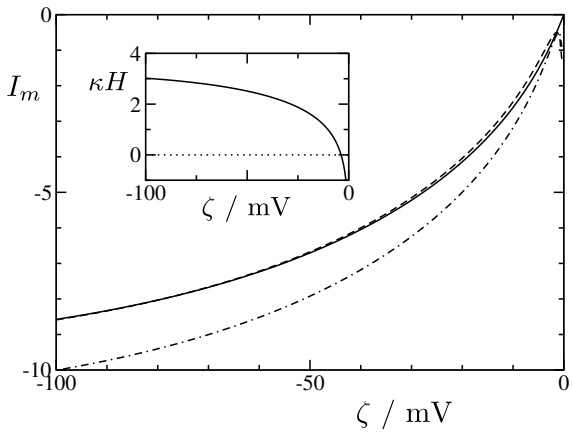


**Fig. 14** The integral $I_m$ evaluated approximately with the method in the text with $\alpha = 1$ (chained line) and $\alpha \approx 0.713$ (dashed line), compared to numerical integration (solid line). The inset shows $\kappa H$ (with $\alpha = 0.713$).

With the intermediate result in Eq. (31), the first two are straightforward. For example,

$$I_1 = \int_0^\infty u\,du\,(e^\psi - 1) = 2\int_0^\infty u\,du\,e^{\psi/2}\sinh\tfrac{1}{2}\psi \tag{35a}$$

$$= -\int_0^\infty u\,du\,e^{\psi/2}\frac{d\psi}{du} \tag{35b}$$

$$= -\Big[u\cdot 2(e^{\psi/2}-1)\Big]_0^\infty + 2\int_0^\infty du\,(e^{\psi/2}-1) \tag{35c}$$

$$= \int_0^{\psi_0} d\psi\,\frac{e^{\psi/2}-1}{\sinh\frac{1}{2}\psi} = \Big[4\ln(1+e^{\psi/2})\Big]_0^{\psi_0} \tag{35d}$$

$$= 4\ln\tfrac{1}{2}(1+e^{\psi_0/2})\,. \tag{35e}$$

In going from (b) to (c) here, the constant in the integration-by-parts has been judiciously chosen to make the boundary contribution vanish. Later, in changing variables from $u$ to $\psi$, the limits of integration have been flipped introducing an extra minus sign. In a similar vein one obtains $I_2 = 4\ln\frac{1}{2}(1+e^{-\psi_0/2})$.

Now we turn to the micelle contribution, codified in $I_m$. As noted in the main text we start by dividing the integration range into inner and outer regions so that

$$I_m = \int_0^{\kappa H} u\,du\,(e^{z\psi}-1) + \int_{\kappa H}^\infty u\,du\,(e^{z\psi}-1) \tag{36a}$$

$$\approx -\tfrac{1}{2}\kappa^2H^2 + \int_{\kappa H}^\infty u\,du\,4zCe^{-u} \tag{36b}$$

$$\approx -\tfrac{1}{2}\kappa^2H^2 + 4zCe^{-\kappa H}(1+\kappa H)\,. \tag{36c}$$

To obtain the intermediate result (b) we suppose that $e^{z\psi} \approx 0$ in the inner region and $e^{z\psi} - 1 \approx z\psi$ in the outer region; then $z \gg 1$ justifies the use of the far-field PBE solution ($\tanh\frac{1}{4}\psi \approx \frac{1}{4}\psi$).

Clearly this approach likely overestimates the inner region and underestimates the outer region. This suggests $\partial I_m/\partial(\kappa H) = 0$ can be used as a criterion to find $\kappa H$, yielding the operational definition $z\psi(\kappa H) = -1$, or $\kappa H = \ln(4z\tanh\frac{1}{4}|\psi_0|)$ noting $z \gg 1$ and $\psi_0 < 0$. Injecting this into the above gives

$$I_m \approx -\tfrac{1}{2}\kappa^2H^2 - (1+\kappa H) = -(1+\kappa H + \tfrac{1}{2}\kappa^2H^2)\,. \tag{37}$$

We have noticed a significant improvement can be made by introducing an empirical adjustment factor so that $\kappa H = \ln(4\alpha z\tanh\frac{1}{4}|\psi_0|)$, whilst retaining Eq. (37) for $I_m$. Choosing $\alpha \approx 0.713$ (as in the main text) produces almost perfect agreement with the numerically-evaluated integral, for relevant parameter ranges (Fig. 14). This approximation for $I_m$ only makes sense if $\kappa H > 0$, which translates into the requirement that $\alpha z|\psi_0| \gtrsim 1$ (for $z \gg 1$). For all practical purposes, this is always satisfied (see for example Fig. 14 inset). It does however generate an artefact at $|\psi_0| \to 0$, which accounts for the unphysical downturn in $I_m$ in this region (Fig. 13).

## Notes and references


1 D. Velegol, A. Garg, R. Guha, A. Kara and M. Kumara, *Soft Matter*, 2016, **12**, 4686–4703.
2 B. V. Derjaguin, G. P. Sidorenkov, E. A. Zubashchenkov and E. V. Kiseleva, *Kolloidn. Zh.*, 1947, **9**, 335–4.
3 E. Ruckenstein, *J. Colloid Interface Sci.*, 1981, **83**, 77–81.
4 D. C. Prieve, *Adv. Colloid Interface Sci.*, 1982, **16**, 321–335.
5 D. C. Prieve, J. L. Anderson, J. P. Ebel and M. E. Lowell, *J. Fluid Mech.*, 1984, **148**, 247–269.
6 J. L. Anderson, *Ann. N. Y. Acad. Sci.*, 1986, **469**, 166.
7 J. P. Ebel, J. L. Anderson and D. C. Prieve, *Langmuir*, 1988, **4**, 396–406.
8 J. L. Anderson, *Ann. Rev. Fluid Mech.*, 1989, **21**, 61.
9 P. O. Staffeld and J. A. Quinn, *J. Colloid Interface Sci.*, 1989, **130**, 69–87.
10 B. Abécassis, C. Cottin-Bizonne, C. Ybert, A. Ajdari and L. Bocquet, *Nat. Mater.*, 2008, **7**, 785–789; see also D. C. Prieve, *Nat. Mater.*, 2008, **7**, 769–770.
11 R. A. Rica and M. Z. Bazant, *Phys. Fluids*, 2010, **22**, 112109.
12 J. Palacci, C. Cottin-Bizonne, C. Ybert and L. Bocquet, *Soft*

*Matter*, 2012, **8**, 980–994.
13 A. Reinmüller, H. J. Schöpe and T. Palberg, *Langmuir*, 2013, **29**, 1738–1742.
14 A. Brown and W. Poon, *Soft Matter*, 2014, **10**, 4016–4027.
15 D. Florea, S. Musa, J. M. Huyghe and H. M. Wyss, *Proc. Natl. Acad. Sci. USA*, 2014, **111**, 6554–6559.
16 A. Kar, T.-Y. Chiang, I. O. Rivera, A. Sen and D. Velegol, *ACS Nano*, 2015, **9**, 746–753.
17 J. S. Paustian, C. D. Angulo, R. Nery-Azevedo, N. Shi, A. I. Abdel-Fattah and T. M. Squires, *Langmuir*, 2015, **31**, 4402.
18 A. Banerjee, I. Williams, R. N. Azevedo, M. E. Helgeson and T. M. Squires, *Proc. Natl. Acad. Sci. USA*, 2016, **113**, 8612–8617.
19 S. Musa, D. Florea, H. M. Wyss and J. M. Huyghe, *Soft Matter*, 2016, **12**, 1127–1132.
20 S. Shin, E. Um, B. Sabass, J. T. Ault, M. Rahimi, P. B. Warren and H. A. Stone, *Proc. Natl. Acad. Sci. USA*, 2016, **113**, 257–261.
21 A. Brown, W. Poon, C. Holm and J. De Graaf, *Soft Matter*, 2017, **13**, 1200–1222.
22 S. Shin, J. T. Ault, J. Feng, P. B. Warren and H. A. Stone, *Adv. Mater.*, 2017, **29**, 1701516.
23 S. Shin, O. Shardt, P. B. Warren and H. A. Stone, *Nat. Commun.*, 2017, **8**, 15181.
24 S. Shin, J. T. Ault, P. B. Warren and H. A. Stone, *Phys. Rev. X*, 2017, **7**, 041038.
25 R. Guha, F. Mohajerani, A. Mukhopadhyay, M. D. Collins, A. Sen and D. Velegol, *ACS Appl. Mater. Interfaces*, 2017, **9**, 43352–43362.
26 S. M. Friedrich, J. M. Burke, K. J. Liu, C. F. Ivory and T.-H. Wang, *Nat. Commun.*, 2017, **8**, 1213.
27 D. C. Prieve, S. M. Malone, A. S. Khair, R. F. Stout and M. Y. Kanj, *Proc. Natl. Acad. Sci. USA*, 2018.
28 R. P. Sear and P. B. Warren, *Phys. Rev. E*, 2017, **96**, 062602.
29 R. Nery-Azevedo, A. Banerjee and T. M. Squires, *Langmuir*, 2017, **33**, 9694–9702.
30 S. Shin, P. B. Warren and H. A. Stone, *Phys. Rev. Appl.*, 2018, **9**, 034012.
31 R. M. Weinheimer, D. Fennell Evans and E. L. Cussler, *J. Colloid Interface Sci.*, 1981, **80**, 357–368.
32 D. F. Evans, S. Mukherjee, D. J. Mitchell and B. W. Ninham, *J. Colloid Interface Sci.*, 1983, **93**, 184–204.
33 D. O. Leaist, *J. Colloid Interface Sci.*, 1986, **111**, 230–239.
34 H. J. Keh and Y. K. Wei, *Langmuir*, 2000, **16**, 5289–5294.
35 N. Kamenka, B. Lindman and B. Brun, *Colloid Polym. Sci.*, 1974, **252**, 144–152.
36 T. G. Movchan, A. I. Rusanov and E. V. Plotnikova, *Colloid J.*, 2016, **78**, 785–794.
37 E. A. G. Aniansson and S. N. Wall, *J. Phys. Chem.*, 1974, **78**, 1024–1030.
38 D. R. Hafemann, *J. Phys. Chem.*, 1965, **69**, 4226–4231.
39 H. J. Hickman, *Chem. Eng. Sci.*, 1970, **25**, 381–398.
40 J. L. Jackson, *J. Phys. Chem.*, 1974, **78**, 2060–2064.
41 V. M. Aguilella, S. Mafé and J. Pellicer, *Electrochim. Acta*, 1987, **32**, 483–488.
42 S. Ghosal and Z. Chen, *Proc. R. Soc. A*, 2010, **466**, 2145–2154.
43 Technically, charge neutrality implies only that $\nabla \cdot \mathbf{I} = 0$ but this can be lifted to $\mathbf{I} = 0$ by noting that all concentration gradients are parallel to each other under the assumption of local equilibrium.
44 S. Lapenna, A. R. Bilia, G. A. Morris and M. Nilsson, *J. Pharm. Sci.*, 2009, **98**, 3666–3675. These experiments are in $D_2O$, so for the data points in Fig. 5 the reported $D_s$ values are multiplied by 1.25 as an empirical correction for the viscosity difference between $D_2O$ and $H_2O$, assuming $D_s\eta \approx$ constant.
45 H. H. von Grünberg, R. van Roij and G. Klein, *Europhys. Lett.*, 2001, **55**, 580–586.
46 R. P. Sear and P. B. Warren, *J. Chem. Phys.*, 2002, **117**, 8074–8079.
47 D. Stigter, R. J. Williams and K. J. Mysels, *J. Phys. Chem.*, 1955, **59**, 330–335.
48 D. C. Prieve and R. Roman, *J. Chem. Soc. Faraday Trans. 2*, 1987, **83**, 1287–1306.
49 K. Shinoda and E. Hutchinson, *J. Phys. Chem.*, 1962, **66**, 577–582.
50 D. G. Hall, *J. Chem. Soc. Faraday Trans. 1*, 1981, **77**, 1121–1156.
51 R. F. Kamrath and E. I. Franses, *Ind. Eng. Chem. Fundamen.*, 1983, **22**, 230–239.
52 J. N. Israelachvili, *Intermolecular and Surface Forces, 3rd edition*, Elsevier, Amsterdam, 2011.